JOURNAL OF MATERIALS SCIENCE 31 (1996) 4913–4920

Phase equilibrium, microstructure and properties of some magnesite–chromite refractories

M.A. SERRY, A.G.M. OTHMAN, L.G. GIRGIS
Ceramic Department, National Research Centre, Dokki, Cairo, Egypt
W. WEISWEILER
Institute of Chemical Technology, University of Karlsruhe, D-76128 Karlsruhe, Germany

The effect of phase equilibrium and microstructure of magnesite–chromite batches containing from 0 to 100% Egyptian chrome ore, with intervals of 10%, on their physical properties was studied. The phase equilibrium data were calculated using the phase relationships within the system M–M_2S–CMS–MR (M = MgO, S = SiO_2, C = CaO, R = R_2O_3). A computerized electron-probe microanalyser was applied to study the microstructure as well as microchemistry of the fired magnesite–chromite co-clinkers. Some physical and technological properties of the co-clinkered briquettes were also investigated by determining densification parameters, spalling resistance and load-bearing capacity.

It is concluded that dense, spalling resistant and refractory magnesite, magnesite–chrome and chrome–magnesite refractories could be produced by co-clinkering of magnesite–chromite batches of 100:0, 70:30 and 30:70 weight ratios, respectively, at 1600 °C. The prepared co-clinkers were subsequently graded, moulded and refired up to 1700 °C in order to obtain direct-bonded bricks. Meanwhile, dense chromite refractories with lower refractory quality could be processed by firing the Egyptian chrome ore up to 1600 °C.

1. Introduction

Composite magnesite–chromite bricks are basic refractories which were used successfully in lining open-hearth roofs and for the clinkering zone of rotary cement kilns. For about three decades the conventional types of these refractories, that were suffering from bursting expansion in service, have been replaced by the direct-bonded bricks. The new type of bricks exhibits a variable degree of direct periclase–periclase and periclase–spinel bonding, replacing partially the silicate matrix of the conventional types. The direct bonding is developed on cooling by precipitation of exsolved spinel in the periclase and/or by crystallization of secondary periclase and spinel from solution in the liquid silicates that formed at the highest firing temperatures [1–3].

The direct-bonded magnesite–chromite refractories are produced by hard firing up to 1800 °C in order to develop refractory solid solution bonds between periclase and spinel. Also, purer magnesite and/or chrome ores with controlled lime/silica ratio are required in order to reduce the amount of interstitial liquid phase and to provide more refractory bonds. However, in commercial bricks containing significant amounts of silica and lime, direct bonding may predominate at relatively lower temperatures of 1700 °C or below [4–6].

The microstructure of magnesite–chromite bricks plays a decisive role in controlling their properties and performance. Generally, as the degree of direct bonding enhances, the mechanical and refractory properties are consequently improved. Magnesite–chromite bricks with a high degree of direct bonding are characterized by high hot temperature strength, improved resistance to slag attack and dimensional stability at temperatures as high as 1800 °C [7–10].

The aim of the present work is to study the phase equilibrium and microstructure of some magnesite–chromite batches and their effect on the technological properties of the fired briquettes. The phase composition in the solid state and the liquid phase contents that could be formed in the fired batches were calculated. The microstructure and microchemistry of the fired samples were investigated using a computerized X-ray electron-probe microanalyser (EPMA). The physical and technological properties by means of densification parameters, thermal shock resistance and load-bearing capacity, were determined. The effect of phase equilibrium and microstructure on the technological properties of the fired briquettes was discussed.

2. Experimental procedure

As materials, dead-burned Turkish magnesite and Egyptian chrome ore were used in this investigation. These materials were both finely ground in a steel ball mill to pass a 0.1 mm sieve. Eleven batches were

0022–2461

prepared by adding chrome ore to the dead-burned magnesite from 0 to 100 mass % with an interval of 10%. The prepared batches were wet mixed, dried and semi-dry pressed into 5-cm cubes under a load of 100 N mm^{-2}. The formed pellets were dried overnight at 110 °C and subsequently co-clinkered for 1 h at 1600 °C. The densification parameters of the fired magnesite–chromite co-clinkers were determined by means of bulk density and apparent porosity using the paraffin displacement method [3].

Two samples of magnesite–chromite co-clinkers, containing 30 and 70% chrome ore, were selected to represent magnesite–chrome and chrome–magnesite refractories, respectively. The selected clinkers, as well as magnesite and chromite clinkers, were separately crushed, graded, mixed and semi-dry pressed to prepare test briquettes from each clinker. Grain batches of 55% coarse (2–0.25 mm), 15% medium (0.25–0.1 mm) and 30% fine (<0.1 mm) were mixed and semi-dry pressed into cylinders of 2.5 cm diameter and about 2.5 cm height under 100 N mm^{-2} pressure. The prepared briquettes were dried and refired for 1 h at 1600 and 1700 °C.

The phase equilibrium, microstructure and properties of the fired briquettes were investigated. The solid phase composition was calculated according to White [13] and quantitatively determined by X-ray diffraction (XRD). The amounts of liquid phase that would develop on firing such clinkers up to 1600 °C were calculated from the available phase relationships given by Solacolu [14]. The microstructure was studied, after gradual polishing of sample surfaces and its coating with a carbon thin film for achieving electrical conductivity, using a computerized electron-probe microanalyser of type CAMEBAX SX 50 attached with an energy dispersive detecting system (EDS) for tracing light elements. The overall picture of microstructure was revealed by back-scattered electron images (BSE), on which line scans for individual elements were superimposed to show qualitatively its distribution within the microstructure. The properties of the studied briquettes in terms of densification parameters, thermal shock resistance and load-bearing capacity were also determined. The results were interpreted in the light of phase composition and microstructure of the magnesite–chromite samples.

3. Results and discussion

Table I summarizes the calculated chemical as well as phase compositions of the magnesite–chromite batches which referred to as MK 1, MK 2, ... MK 11. The solid phase composition is calculated according to White [13], assuming that the equilibrium conditions have been attained on firing these batches in normal atmosphere up to 1600 °C. Also, the liquid phase content that would be developed at 1600 °C is calculated according to Solacolu [14]. It is evident that Turkish magnesite (MK 1) has about 94 mass % MgO and the other oxides are SiO_2, CaO and R_2O_3 in decreasing order of abundance. The addition of Egyptian chromite to magnesite, at 10% interval up to 90% (MK 10), leads to a gradual increase of R_2O_3 and

TABLE I Chemical and phase composition of magnesite–chromite batches

Batch	Batch composition		Chemical composition (mass %)					CaO/SiO_2 molar ratio	Phase composition (mass %)					Liquid phase content (mass %) at 1600 °C
	Magnesite	Chromite	SiO_2	Cr_2O_3	Fe_2O_3	Al_2O_3	CaO	MgO		CMS	M_2S	MK	MF	MA	MgO	
MK 1	100	–	2.99	0.06	0.48	0.24	2.16	94.07	0.78	6.02	1.57	0.08	0.60	0.34	91.40	15.7
MK 2	90	10	3.39	4.59	1.85	1.61	2.08	86.48	0.66	5.79	2.71	5.80	2.31	2.24	81.14	21.4
MK 3	80	20	3.79	9.12	3.22	2.96	2.02	78.89	0.57	5.63	3.79	11.52	4.02	4.12	70.92	23.8
MK 4	70	30	4.19	13.65	4.59	4.33	1.94	71.30	0.50	5.40	4.93	17.24	5.86	5.40	60.66	25.3
MK 5	60	40	4.59	18.19	5.96	5.69	1.87	63.70	0.44	5.21	6.08	22.98	7.45	7.92	50.40	27.7
MK 6	50	50	4.99	22.72	7.33	7.05	1.80	56.11	0.39	5.01	7.16	28.70	9.16	9.81	40.16	29.5
MK 7	40	60	5.39	27.24	8.70	8.42	1.72	48.52	0.34	4.79	8.28	34.41	10.88	11.72	29.92	29.8
MK 8	30	70	5.79	31.78	10.07	9.78	1.65	40.93	0.31	4.60	9.38	40.15	12.58	13.62	19.68	30.3
MK 9	20	80	6.19	36.31	11.44	11.15	1.57	33.33	0.27	4.37	10.53	45.87	14.30	15.52	9.41	30.8
MK10	10	90	6.59	40.84	12.81	12.50	1.51	25.75	0.25			not calculated				–
MK11	–	100	6.99	45.37	14.18	13.87	1.43	18.15	0.22			not calculated				–

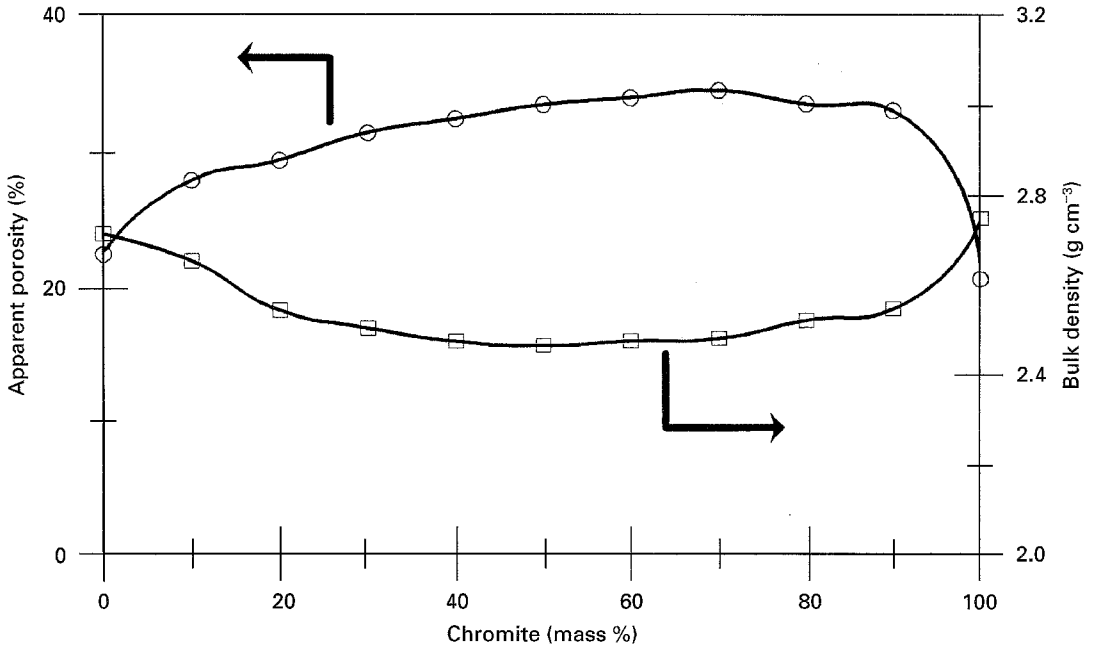

Figure 1 Densification curves of magnesite–chromite co-clinker fired at 1600 °C.

SiO_2 contents of the batches at the expense of their contents of MgO and CaO. The Egyptian chrome ore (MK 11) has a higher Cr_2O_3 content (45.4%) relative to the iron oxides as Fe_2O_3 (14.2%) and Al_2O_3 (13.9%) contents. It contains also higher SiO_2 (7.0%) and CaO (1.4%) than those of the well-known chrome ores [1–3].

The CaO/SiO_2 molar ratio of all batches (MK 1 to MK 11) is less than 1. Therefore, its solid-phase composition comprises: monticellite (CMS), forsterite (M_2S), spinel solid solution (MR) and free MgO, except MK 10 and MK 11 batches which contain excess Fe_2O_3 and/or Al_2O_3 and no free MgO [13]. Hence, the phase composition of the latter batches could not be calculated. From Table I it is also illustrated that as the addition of chrome ore is increased up to 80% (MK 9), more forsterite is formed at the expense of monticellite due to the subsequent decrease of its CaO/SiO_2 ratio. Meanwhile, the amount of spinel solid solution (MK–MF–MA) is increased at the expense of free periclase, by increasing the addition of chromite. This leads to the gradual development of liquid phase content from 15.7% in magnesite (MK 1) up to 30.3% in MK 9, as calculated by plotting the studied compositions by means of their moduli of calcia and silica on the modular system given by Solacolu [14] for the phase diagram of the $MgO–M_2S–CMS–MR$ subsystem.

Fig. 1 exhibits the densification curves of the magnesite–chromite co-clinkers fired at 1600 °C as a function of chromite content. It is evident that the addition of chromite up to 30% gradually deteriorates the densification process, as indicated from the lower bulk density and the higher apparent porosity shown by sample MK 4, as compared with magnesite (MK 1). The increase of chromite content up to 70% leads to a slight deterioration of densification. This is mainly attributed to the bursting expansion that occurs during firing magnesite–chromite batches with the formation of discrete pores [15, 16]. These pores are formed during the recrystallization of spinel solid solution (s.s.) as a result of the unequal diffusion rates of its components. At temperatures higher than 1000 °C, iron oxides (Fe^{2+} and Fe^{3+}) occupy both tetrahedral

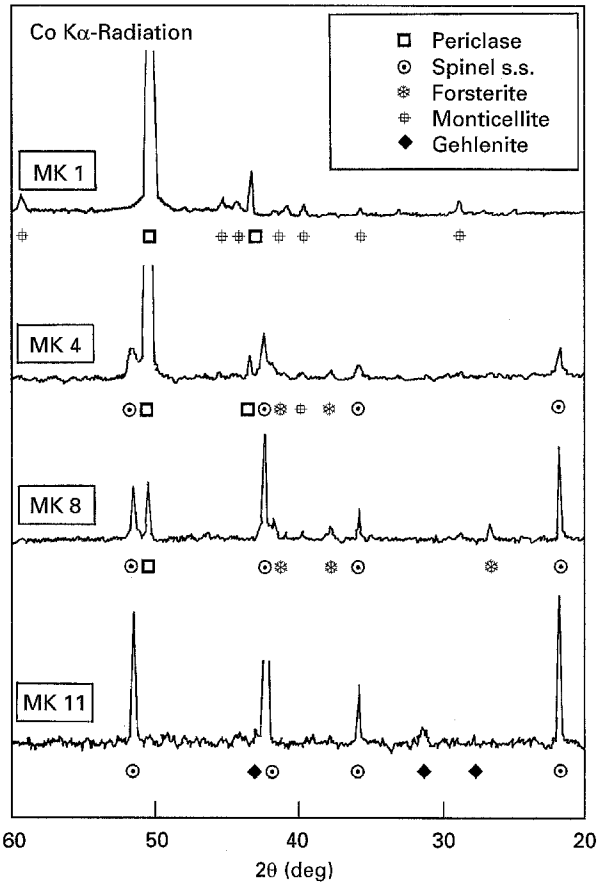

Figure 2 XRD patterns of magnesite (MK 1), magnesite–chrome (MK 4), chrome–magnesite (MK 8) and chromite (MK 11) co-clinkers fired at 1600 °C.

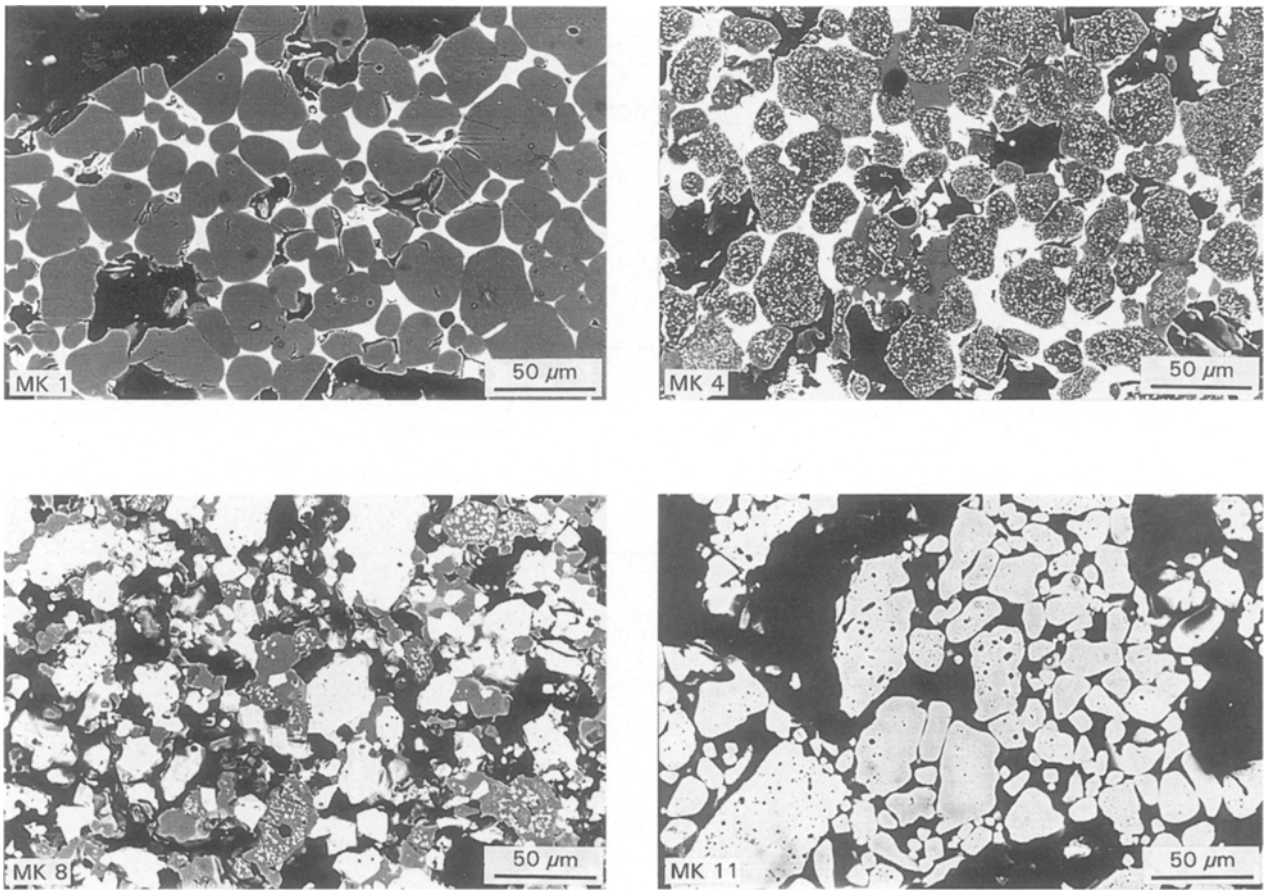

Figure 3 Back-scattered electron images (BSE) of magnesite (MK 1), magnesite–chrome (MK 4), chrome–magnesite (MK 8) and chromite (MK 11) co-clinkers fired at 1600 °C.

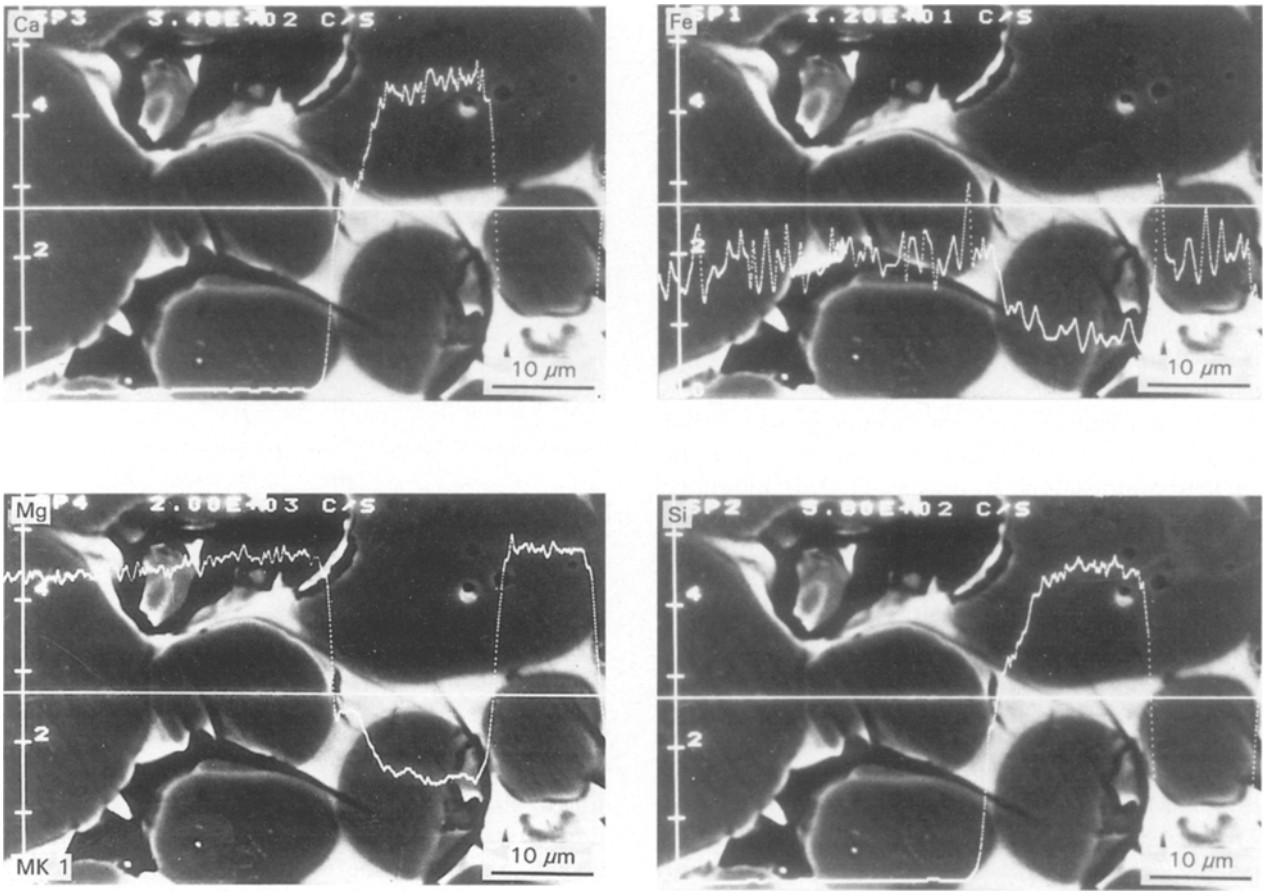

Figure 4 Line scans for Mg, Fe, Ca and Si superimposed on BSE images of magnesite clinker (MK 1).

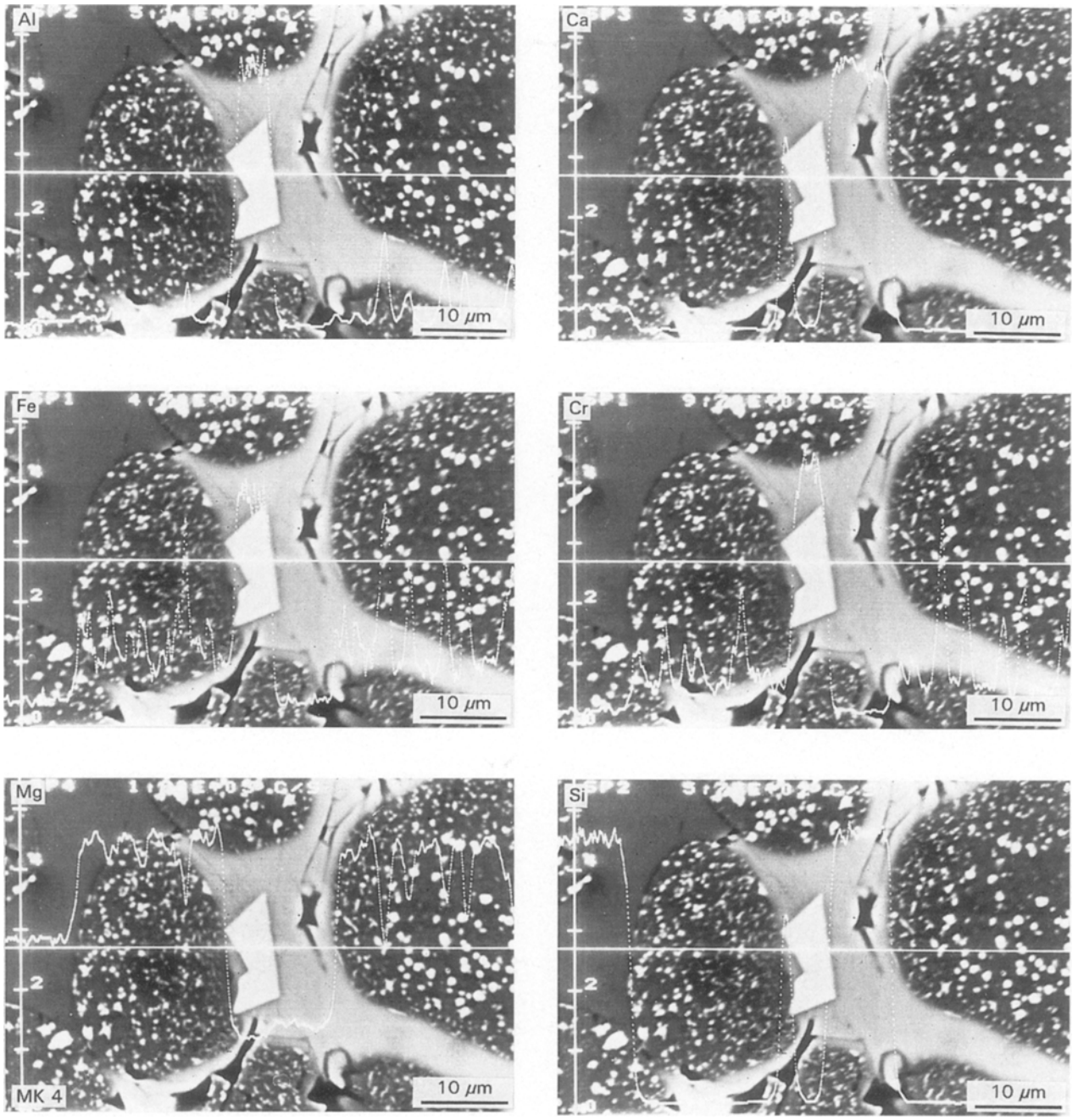

Figure 5 Line scans for Mg, Cr, Fe, Al, Ca and Si superimposed on BSE images of magnesite-chrome co-clinker (MK 4).

and octahedral positions in the spinel lattice, whereas Cr^{3+} ions occupy only its octahedral positions [15, 16]. Hence, iron ions diffuse faster than Cr^{3+} ions, and the firing of magnesite–chromite batches up to 1600 °C leads to the formation of discrete pores with the deterioration of its densification. This deterioration occurs rapidly on increasing chromite content up to 30% and then steadily up to 70% chromite, as shown in Fig. 1. On raising the chromite content up to 100%, a gradual improvement in densification is evident. This is mainly due to the insufficient magnesite (MgO) content required for the reaction with the sesquioxides of chrome ore to form spinel s.s. phase. Hence, excess free sesquioxides, namely Fe_2O_3 and/or Al_2O_3, coexist with the spinel s.s. phase, leading to the development of higher liquid phase contents that participate in the densification of magnesite–chromite batches containing 80, 90 and 100% chromite [14–16]. According to the above results, magnesite–chromite batches containing 30% (MK 4) and 70% (MK 8) chrome ore are selected to represent magnesite–chrome and chrome–magnesite refractories for further investigations in comparison with magnesite (MK 1) as well as chromite (MK 11) samples.

Fig. 2 shows the XRD patterns of the selected magnesite–chromite co-clinkers MK 1, MK 3, MK 8 and MK 11. These patterns confirm the calculated phase composition as given in Table I. Magnesite (MK 1) composes mainly of periclase in addition to some lines of monticellite. Also MK 4 (magnesite–chrome) is composed mainly of periclase with some spinel s.s., whereas spinel s.s. becomes predominant in MK 8 (chrome–magnesite) with some periclase and forsterite phases. Forsterite and monticellite phases are

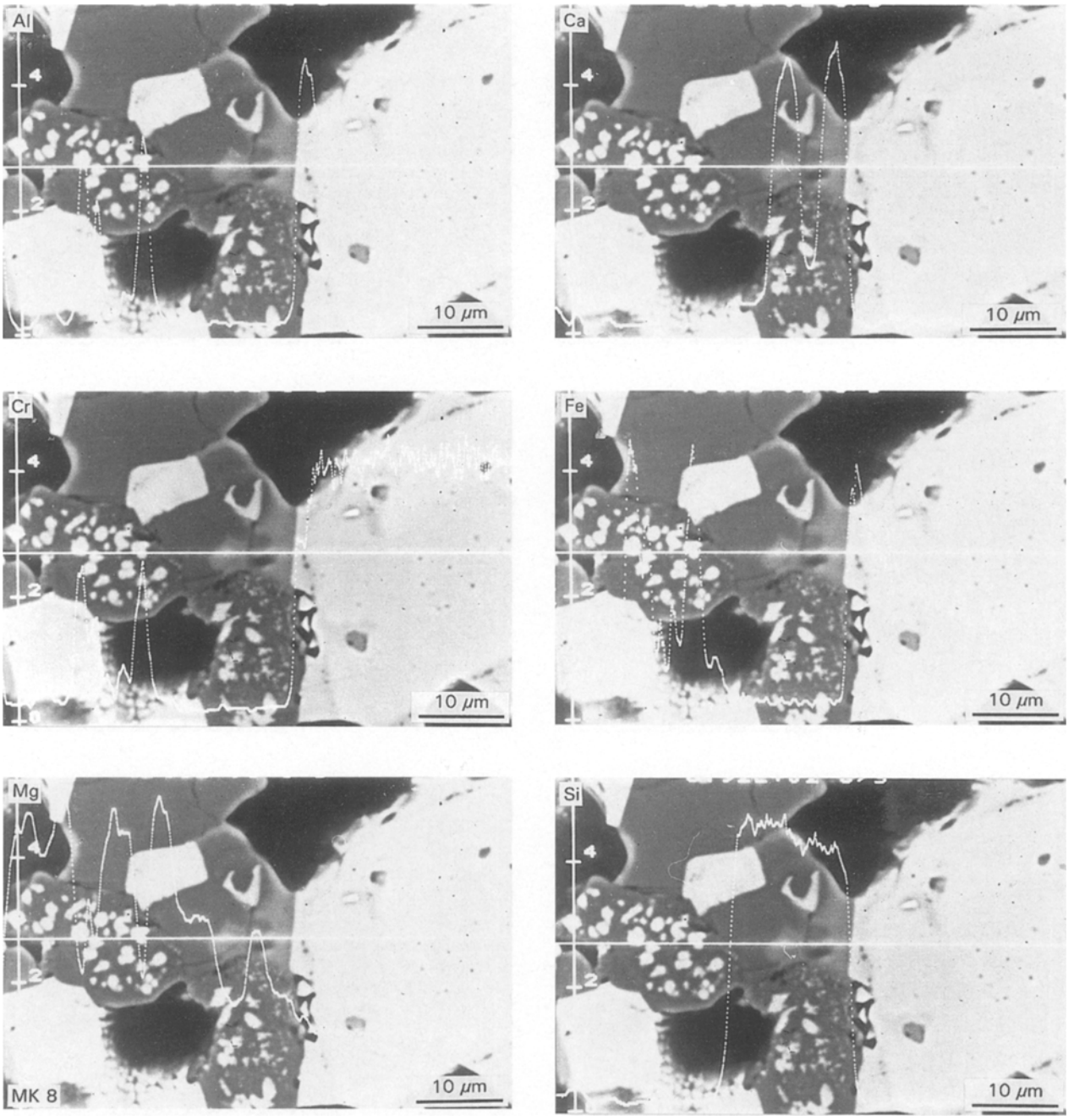

Figure 6 Line scans for Mg, Cr, Fe, Al, Ca and Si superimposed on BSE images of chrome-magnesite co-clinker (MK 8).

also detected in MK 3 and MK 8. Meanwhile, fired chromite (MK 11) is mainly composed of spinel s.s. in addition to some gehlenite (C_2AS) phase. The formation of the latter phase may be due to excess Al_2O_3 and Fe_2O_3 over that required for spinel solid solution on firing up to 1600 °C. This leads to the reaction of surplus Al_2O_3 and Fe_2O_3 with CaO and SiO_2 to form gehlenite phase [10].

Figs 3–7 exhibit the microstructure and microchemistry of MK 1, MK 4, MK 8 and MK 11 clinkers as shown from the secondary electron images obtained by the electron-probe microanalyser. Fig. 3 shows the overall microstructure of the clinker samples whereas Figs 4, 5, 6 and 7 illustrate the distribution of chemical constituents within the phases of samples MK 1, MK 4, MK 8 and MK 11, respectively.

From Figs 3(a) and 4 it is shown that magnesite clinker (MK 1) is composed mainly of rounded to subrounded periclase grains (dark) of variable sizes having an appreciable degree of direct bonding. The periclase grains are bonded with a calcium–magnesium silicate phase (bright) which is detected by XRD (Fig. 2) as monticellite. Both the periclase and monticellite phases contain some iron oxides in solid solution with higher content in periclase, as is evident from Fig. 4.

Figs 3(b) and 5 show fine spinel solid solution particles (bright) precipitated within the periclase grains of the magnesite–chrome sample (MK 4). The matrix is composed of monticellite (bright) and forsterite (grey) enclosing some secondary euhedral spinel crystals which contain relatively higher Al_2O_3, and lower Cr_2O_3 and Fe_2O_3, than the spinel s.s. precipitated as ex-solution inside the periclase. This is mainly due to the lower rate of dissolution of Al_2O_3 in the periclase as compared with Cr_2O_3 and Fe_2O_3 in the chrome ore

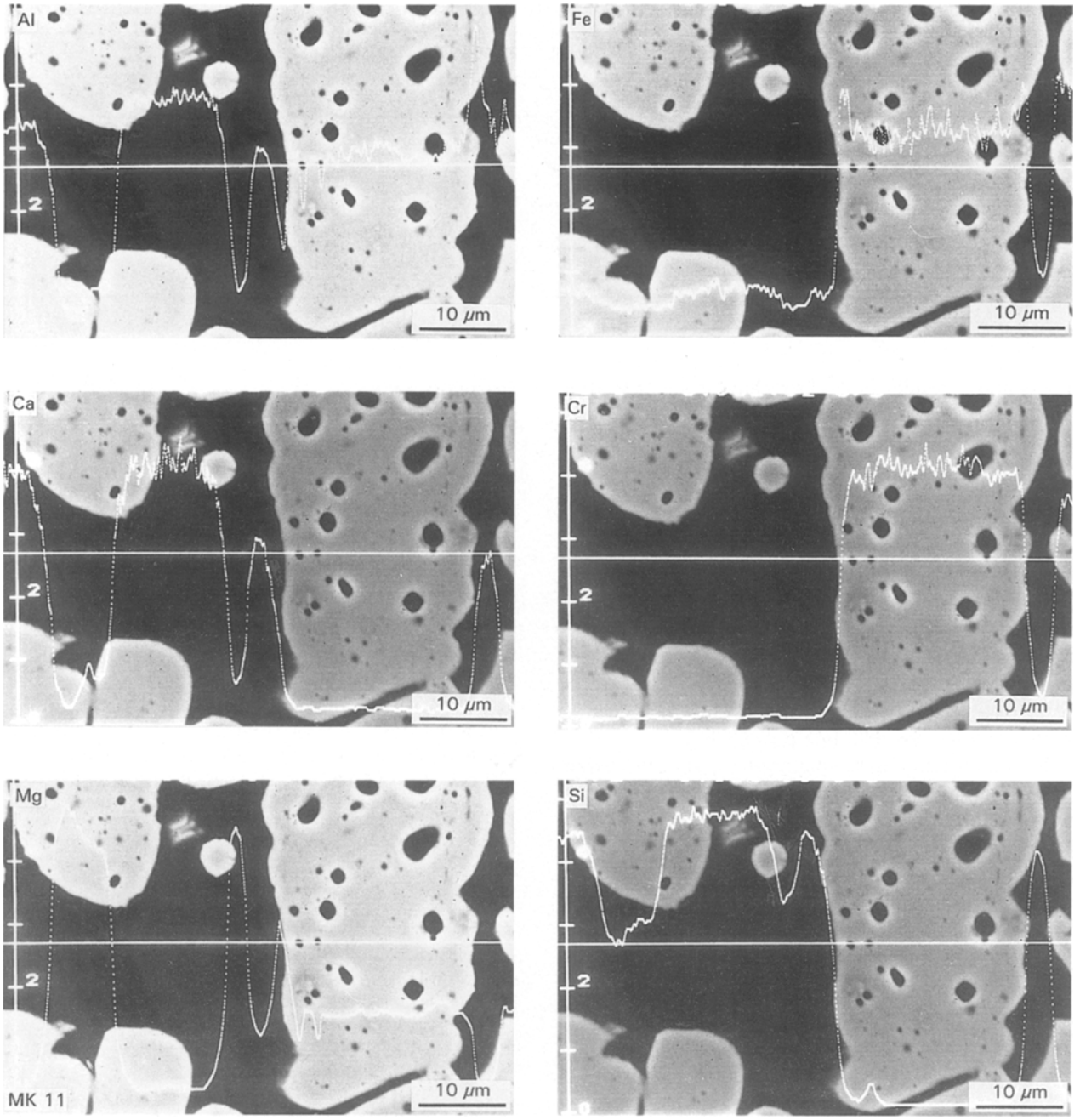

Figure 7 Line scans for Mg, Cr, Fe, Al, Ca and Si superimposed on BSE images of chromite clinker (MK 11).

[16]. Therefore, more Al_2O_3 has existed in the silicate liquid phase at 1600 °C from which the secondary spinel s.s. phase is crystallized on cooling.

The microstructure and microchemistry of the chrome–magnesite sample (MK 8) is exhibited in Figs 3(c) and 6, respectively. From these figures it is shown that spinel solid solution grains with variable sizes are predominant and bonded mainly by periclase s.s. and forsterite phases. Some minor monticellite phase is also detected. The higher amount of calcium and/or magnesium silicate phases present in the latter sample, as well as the relatively lower firing temperature are responsible for the very low degree of direct bonding shown between spinel s.s. and periclase phases [16]. It is also interesting to note here that the concentration of iron oxides is higher at spinel-grain edges than at its centre as previously reported [16, 17].

The chromite sample (Fig. 7) shows rounded to subrounded spinel grains with variable sizes, having a very low degree of direct bonding. Calcium aluminium silicate and magnesium silicate phases (black) exist in the interstitial spaces of the spinel grains which enclose some rounded pores due to its discontinuous grain growth in the presence of liquid phase [15]. This liquid contains higher amounts of Al_2O_3 and Fe_2O_3 together with CaO, MgO and SiO_2. Therefore, $2CaO–Al_2O_3–SiO_2$ (gehlenite), as well as $2MgO–SiO_2$ (forsterite) phases containing some iron in solid solution, are recrystallized from such a liquid phase on cooling. This is confirmed by the results of XRD, as shown in Fig. 2.

The densification properties, thermal shock resistance and load-bearing capacity of briquettes made from the selected magnesite–chromite co-clinkers and fired at 1600 and 1700 °C are summarized in Table II.

TABLE II Properties of magnesite–chromite briquettes fired at 1600 and 1700 °C

Properties	MK 1		MK 4		MK 8		MK 11	
	1600 °C	1700 °C	1600 °C	1700 °C	1600 °C	1700 °C	1600 °C	1700 °C
Bulk density (g cm^{-3})	2.60	2.91	2.59	3.18	2.57	3.24	3.18	–
Apparent porosity (%)	23.3	15.0	23.4	8.6	28.7	10.3	0.50	–
Thermal shock resistance (No. of cycles)	+ 20	+20	+ 20	+ 20	+ 20	+ 20	+ 20	–
Temperature corresponding to the beginning of subsidence: T_a (°C)	> 1500	> 1500	1470	> 1500	1450	> 1500	1370	–

From these results it is clear that the densification parameters and the load-bearing capacity of the magnesite (MK 1), magnesite–chrome (MK 4) and chrome–magnesite (MK 8) briquettes are appreciably improved by raising the firing temperature from 1600 to 1700 °C. This indicates that these briquettes should be fired at temperatures higher than 1700 °C in order to enhance the direct-bonding effect of such briquettes containing high amounts of lime and silica [1–10]. Meanwhile, dense chromite briquettes of low refractory quality could be produced by firing MK 11 briquettes at 1600 °C. The high thermal shock resistance of all briquettes studied is mainly due to its coarse grading with only 30% fine powder [1].

In conclusion, dense, spalling-resistant and refractory magnesite, magnesite–chrome and chrome–magnesite refractories could be produced by firstly co-clinkering of magnesite–chromite batches of 100:0, 70:30 and 30:70 weight ratios, respectively, at 1600 °C, and secondly by subsequently grading the prepared co-clinkers, then moulding and firing at 1700 °C in order to produce direct-bonded bricks. On the other hand, dense chromite refractories with low grade could be manufactured by firing the Egyptian chrome ore up to 1600 °C.

Acknowledgement

The authors are greatly indebted to the Ministry of Science and Art, Stuttgart/Germany, to the German Academic Exchange Organization (DAAD), Bonn and to the International Seminar, Karlsruhe University, Karlsruhe/Germany for the financial support and facilities provided to conduct this work.

References

1. J. LAMING, in "High temperature oxides", Vol. 1, edited by A. M. Alper (Academic Press, New York and London, 1970) p. 143.
2. H. M. KRANER, in "Phase diagrams, materials science and technology", Vol. 11, edited by A. M. Alper (Academic Press, New York and London, 1970) p. 67.
3. J. H. CHESTERS, "Refractories, production and properties" (Iron and Steel Institute, London, 1973).
4. A. HAYHURST and J. LAMING, *Refractories J.* **39** (1963) 80–84, 90, 94, 96, 115.
5. J. LAMING, *Refractories J.* **35** (1959) 116.
6. B. JACKSON and W. F. FORD, *Trans. Brit. Ceram. Soc.* **65** (1966) 19.
7. M. I. VAN DRESER and W. H. BOYER, *J. Amer. Ceram. Soc.* **46** (1963) 257.
8. B. DAVIES and F. H. WALTHER, *Ibid.* **47** (1964) 116.
9. P. E. SCHEERER, H. M. MIKAMI and J. A. TAUBER, *Ibid.* **47** (1964) 297.
10. J. WHITE, *Refractories J.* **46** (1970) 6.
11. S. N. RUDDLESDEN, *Proc. Brit. Ceram. Soc.* **20** (1972) 1.
12. W. PIATKOWSKI, *Ceramurgia Int.* **2** (1976) 38.
13. J. WHITE, in "High temperature oxides", Vol. 1, edited by A. M. Alper (Academic Press, New York and London, 1970) p. 77.
14. S. SOLACOLU, *Berichte DKG* **37** (1960) 266.
15. G. R, RIGBY, *Trans. Brit. Ceram. Soc.* **55** (1956) 22.
16. R. G. RICHARDS, A. GUNN and N. E. DOBBINS, *Ibid.* **55** (1956) 507.
17. J. D. DEWENDRA, C. M. WILSON and N. H. BRETT, *Ibid.* **81** (1982) 185; **82** (1983) 64, 87, 132.
18. S. C. KOHN and S. BUTLER, *Ibid.* **84** (1985) 15.
19. D. L. JOHNSON and L. B. CUTHER, in "Phase diagrams, materials science and technology", Vol. 2, edited by A. M. Alper (Academic Press, New York and London, (1970) p. 465.

Received 1 December 1994
and accepted 13 February 1996